ENTHUSIASTIC
INTERNATIONAL JOURNAL OF APPLIED STATISTICS AND DATA SCIENCE
Volume 5, Issue 1, April 2025, pp. 9-19

Temperature Prediction in Norway Using GRUs: A Machine Learning Approach

Andrie Pasca Hendradewa [a, b, 1,*], Dina Tri Utari [c, 2]

[a] Department of Mechanical and Industrial Engineering, Norwegian University of Science and Technology, Verkstedteknisk, P523, Gløshaugen, Richard Birkelands veg 2B, 7034, Trondheim, Norway
[b] Department of Industrial Engineering, Universitas Islam Indonesia, Jalan Kaliurang KM 14.5 Yogyakarta 55584, Indonesia
[c] Department of Statistics, Universitas Islam Indonesia, Jalan Kaliurang KM 14.5 Yogyakarta 55584, Indonesia

[1] andrie.p.hendradewa@ntnu.no*; [2] dina.t.utari@uii.ac.id
* Corresponding author

ARTICLE INFO

ABSTRACT

Keywords
Daily Temperature
GRU-Based Time Series Prediction
Climate Pattern Analysis
Norwegian Regional Temperature Prediction

Accurate temperature forecasting in Norway is significant for environmental stewardship and disaster management, in addition to providing essential support for critical sectors, including agriculture, urban development, and energy resource management. This study employed the gated recurrent unit (GRU) to augment the precision of temporal temperature forecasts. After that, it was used to project temperatures for seven days. The dataset, obtained from https://www.yr.no/nb, comprised records of minimum and maximum temperatures spanning from February 1, 2018, to December 31, 2024. The data was partitioned, with 80% allocated for training and 20% designated for testing. Utilizing a training regimen of 20 epochs alongside a three-day lookback interval, the model attained R^2 scores of 0.82 for minimum temperature predictions and 0.86 for maximum temperature forecasts. These results underscore the GRU model's capacity to accurately capture daily temperature variations and produce dependable predictions. Given its commendable performance on training and testing datasets, the GRU model is particularly suitable for temperature forecasting.

1. Introduction

Climate change and its associated effects have underscored the necessity for precise temperature forecasting. It is an indispensable instrument for tackling the multifaceted challenges inherent in environmental management, agricultural practices, energy resource management, and urban development. The evolving climatic patterns, characterized by an increase in the frequency of extreme meteorological occurrences and temperature deviations, necessitate the implementation of exacting forecasting methodologies to alleviate risks and refine decision-making processes.

Norway, characterized by its heterogeneous climatic zones from coastal regions influenced by the North Atlantic Ocean to its inland and Arctic territories, poses distinctive challenges for temperature forecasting. The nation's intricate topographical features, encompassing fjords,

p-ISSN 2798-253X
e-ISSN 2798-3153

mountainous terrains, and valleys, further complicate predicting temperature variations across its diverse regions. These geographical attributes exert considerable influence on localized weather phenomena, engendering microclimates that necessitate the application of highly localized and sophisticated forecasting methodologies.

The precision of temperature forecasting in Norway is imperative for effective environmental and disaster management and bolstering critical sectors such as agriculture, where accurate temperature information is crucial for strategic crop planning and frost mitigation. Furthermore, urban planning and infrastructure development domains increasingly rely on dependable climate forecasts to efficiently address heating, cooling, and energy requirements. In Norway's Arctic regions, the significance of forecasting is amplified as rising temperatures yield substantial ramifications for sea ice, permafrost integrity, and biodiversity, thereby impacting both local populations and global climatic systems [1], [2]. Recent advancements in statistical techniques and machine learning present promising avenues for augmenting the accuracy of temperature forecasts in Norway. By amalgamating historical climatic data with state-of-the-art modeling approaches, researchers are better equipped to account for the intricate interactions among the myriad factors contributing to temperature fluctuations. This progression harbors the potential to bolster climate resilience and sustainability initiatives nationwide.

Traditional statistical methodologies frequently prove inadequate in elucidating the intricate, nonlinear interrelationships characteristic of meteorological data. Traditional methodologies generally depend on linear assumptions and simplistic frameworks that inadequately capture the intricate nature of environmental phenomena. For example, although linear regression has served as the conventional instrument for delineating relationships among meteorological variables, empirical studies have indicated that this methodology frequently proves inferior to more sophisticated machine learning approaches capable of modeling intricate and multifactorial data interactions [3]–[5]. In response to these limitations, machine learning methodologies, notably gated recurrent unit (GRU), have emerged as formidable instruments for predicting time series, providing enhanced accuracy and efficiency compared to traditional models. As a specific variant of recurrent neural networks (RNNs), GRU is purposefully constructed to adeptly manage sequential data by alleviating complications associated with vanishing gradients, which are typically prevalent in conventional RNN frameworks. GRU streamlines the architecture of long short-term memory (LSTM) networks by integrating the input and forget gates into a singular update gate, thereby diminishing computational complexity whilst preserving performance [6]. This feature renders GRU especially advantageous for applications demanding real-time predictions, such as temperature forecasting, wherein timely and precise data is vital for informed decision-making.

Recent scholarly investigations have elucidated the efficacy of GRUs within diverse contexts of temperature forecasting. For instance, previous research formulated a GRU-based model aimed at short-term forecasting of wind speed and temperature, attaining significant enhancements in predictive accuracy when juxtaposed with conventional methodologies [7]. In a similar vein, other research employed GRU to the predict the sea surface temperature, thereby demonstrating their proficiency in effectively managing sparse datasets and generating dependable forecasts [8]. These results accentuate the potential of GRU to augment temperature prediction models, particularly in regions such as Norway, where environmental conditions exhibit considerable variability. Furthermore, the amalgamation of GRU with supplementary techniques, including attention mechanisms, has yielded further advancements in their predictive capabilities. Attention mechanisms facilitate models in concentrating on pertinent input data segments, thereby enhancing the GRUs capacity to assimilate historical temperature patterns and improving its aptitude for capturing long-term dependencies [9]. This is especially pertinent for temperature forecasting; wherein antecedent weather conditions can substantially influence forthcoming temperatures.

This paper presents an innovative methodology for forecasting temperature variations in Norway by utilizing a model grounded in GRUs. By capitalizing on historic temperature datasets and integrating pertinent meteorological factors, the authors aimed to establish a resilient predictive framework capable of delivering precise and prompt temperature prognostications. While traditional

p-ISSN 2798-253X
e-ISSN 2798-3153

statistical methodologies such as autoregressive–moving-average (ARMA) or autoregression (AR) demonstrate efficacy for stationary and linear datasets, the implementation of GRUs in this scatter explicitly to the intricate, nonlinear, and dynamic characteristics inherent in meteorological data. Temperature fluctuations in Norway reveal pronounced seasonality and circumstances that traditional linear methodologies might frequently fail to encapsulate adequately. GRU proficiently navigates these complexities by effectively capturing long-term dependencies and nonlinear interrelations within sequential data, devoid of stringent stationarity assumptions or the necessity for extensive feature engineering.

Furthermore, GRU proficiently tackles prevalent challenges faced by neural networks, such as the vanishing gradient dilemma, thereby augmenting their capacity to accurately model long-term climatic shifts. Consequently, the originality of this investigation resides in the practical application of GRU-based forecasting to Norwegian temperature datasets, offering a robust and pragmatic alternative to classical methodologies and yielding significant insights for agriculture, energy management, and environmental planning.

2. Materials and Methods

The data used in this study was secondary data obtained from the website https://www.yr.no/nb. The variables included the minimum and maximum temperatures from February 1, 2018, to December 31, 2024. Minimum temperature denotes the lowest temperature documented throughout a designated timeframe, typically assessed during the nocturnal hours or in the early morning when thermal readings are prone to decline. This temperature is of paramount importance for evaluating frost risk, which can profoundly influence agricultural methodologies and crop viability. For example, comprehending the minimum temperature facilitates farmers' implementation of frost mitigation tactics to safeguard sensitive crops against potential damage [10]. Conversely, maximum temperature signifies the highest temperature recorded within the identical timeframe, usually occurring in the afternoon when solar radiation reaches its zenith. Maximum temperatures are essential for assessing heat stress conditions, which can adversely impact both human health and agricultural efficacy. Elevated maximum temperatures can result in increased evaporation rates, affecting water availability for crops and livestock [11], [12].

2.1. Gated Recurrent Unit

GRU is a type of RNN architecture similar to LSTM. Like LSTM, GRU is designed to process sequential data by allowing information to be remembered or forgotten selectively over time. However, the architecture of a GRU is more straightforward than an LSTM, with fewer parameters, making it easier to train and more computationally efficient [13]. GRU consists of interconnected units that can remember information from the past. Fig. 1 depicts the architecture of a GRU, emphasizing its two fundamental gates: the reset gate and the update gate. These gates proficiently regulate the dissemination of information throughout the network, alleviating the vanishing gradient phenomenon frequently observed in artificial neural networks. GRU has been proven effective in various sequential data processing tasks such as speech recognition, natural language modeling, and stock price prediction [14].

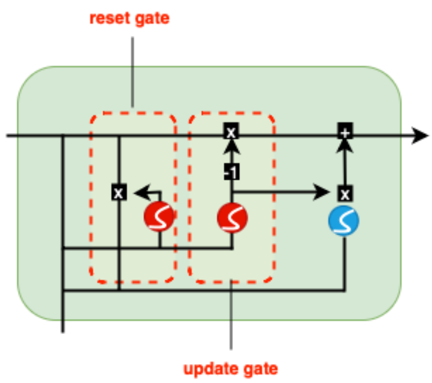

Fig. 1 GRU architecture.

p-ISSN 2798-253X
e-ISSN 2798-3153

A gate is a mechanism used to regulate the flow of information in neural networks. It utilizes a binary sigmoid function (σ) and multiplication operations with input values (x). The binary sigmoid function acts as an enable function that is very effective for processing data with a range of values between 0 and 1.

The reset gate denotes the number of previous gates present. At the same time, the update gate determines the number of candidates it has determined to enter the new hidden state.

Reset gate:

$$r_t = \sigma(W_r[h_{t-1}, x_t] + b_r) \tag{1}$$

Update gate:

$$z_t = \sigma(W_z[h_{t-1}, x_t] + b_z) \tag{2}$$

Hidden state:

$$\tilde{h}_t = \tanh W_h x_t + U_h(r_t \odot h_{t-1}) + b_h \tag{3}$$

$$h_t = (1 - z_t) \odot h_{t-1} + z_t \odot \tilde{h}_t \tag{4}$$

In (1)–(4), σ represents the sigmoid activation function, which maps input values to a range between 0 and 1, thereby controlling the flow of information within the neural network gates. The term x_t denotes the input data at time step t, while $\tilde{h}_t$ refers to the candidate value used for updating the hidden state. The hidden state, indicated by h_t, is the output of the GRU cell at each time step. The parameters of W_r, W_z, and W_h are weight matrices applied to the inputs and previous hidden states during computation. The hyperbolic tangent function, denoted by tanh, introduces nonlinearity to the model, allowing it to learn complex temporal patterns. Lastly, b_r, b_z, and b_h represent bias terms that adjust the activation thresholds for the reset, update, and hidden gates, respectively.

2.2. The Evaluation Metrics

The evaluative metrics, which encompass the mean absolute error (MAE), the mean absolute percentage error (MAPE), the root mean square error (RMSE), and the coefficient of determination (R^2), are indispensable for the appraisal of regression models and various predictive methodologies. Each metric provides distinct perspectives on model efficacy, thereby making comprehending their definitions, formulations, and specific applications vital.

2.2.1. Mean Absolute Error (MAE)

MAE measures the average size of the discrepancies between predicted values and actual outcomes, independent of the sign of these discrepancies. It is determined through (5).

$$MAE = \frac{1}{n}\sum_{i=1}^{n}|y_i - \hat{y}_i| \tag{5}$$

where y_i represents the actual observed value, $\hat{y}_i$ denotes the predicted value, and n signifies the total number of observations. The application of MAE is advantageous as it furnishes a clear interpretation of the average deviation in the same units as the data under consideration, thereby rendering it comprehensible [15], [16].

2.2.2. Mean Square Error (MSE)

MSE is an essential metric within statistical estimation theory. It encapsulates the mean of the squares of discrepancies, specifically, the mean squared deviation between estimated values and their corresponding actual values. This statistical measure is essential across many disciplines, such as signal processing, machine learning, and statistical inference, as it offers a quantitative framework for evaluating the precision of estimators. Mathematically, the MSE is expressed in (6).

$$MSE = \frac{1}{n}\sum_{i=1}^{n}(y_i - \hat{y}_i)^2. \tag{6}$$

MSE evaluates an estimator’s efficacy under conventional conditions and elucidates its intrinsic bias and variance. For example, estimators exhibiting a low MSE possess advantageous characteristics such as consistency and unbiasedness, which are essential for robust statistical inference [17], [18].

p-ISSN 2798-253X
e-ISSN 2798-3153

2.2.3. Root Mean Square Error (RMSE)

RMSE quantifies the square root of the mean of the squared discrepancies between forecasted values and actual measurements:

$$RMSE = \sqrt{\frac{1}{n}\sum_{i=1}^{n}(y_i - \hat{y}_i)^2}. \quad (7)$$

RMSE assigns a disproportionately higher significance to more significant discrepancies owing to the squaring of the deviations, rendering it exceptionally advantageous in scenarios where substantial errors are to be avoided [15], [19]. Its application spans a multitude of disciplines to validate predictive models because of its heightened sensitivity to significant deviations, thereby aiding in the assurance of robustness across various domains, including environmental research and clinical forecasting [20], [21].

2.2.4. Coefficient of Determination (R^2)

R^2 serves as a quantitative measure of the extent to which the independent variables elucidate the variability inherent in the dependent variable, which can be mathematically expressed as in (8).

$$R^2 = 1 - \frac{\sum_{i=1}^{n}(y_i - \hat{y}_i)^2}{\sum_{i=1}^{n}(y_i - \bar{y})^2} \quad (8)$$

where $\bar{y}$ denotes the arithmetic mean of the observed values. An R^2 statistic approaching 1 indicates that a substantial proportion of the variance is elucidated by the independent variables within the constructed model [16], [20]. Despite its prevalent application, caution is warranted in interpreting R^2, as it does not signify a causal relationship and may be artificially enhanced through overfitting.

3. Results and Discussion

Fig. 2 depicts the temperature fluctuations in Norway from February 1, 2018, to December 31, 2024. The graphical representation effectively delineates the seasonal variations, emphasizing a pronounced cyclical trend in minimum and maximum temperature readings.

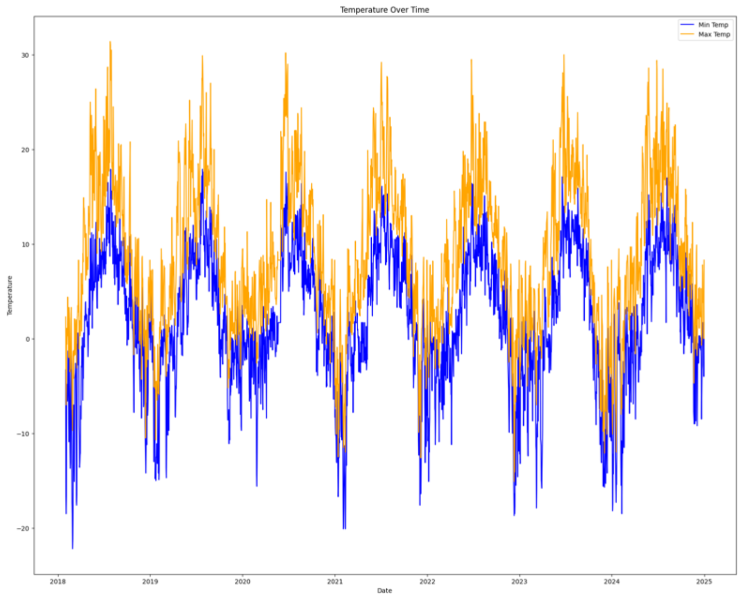

Fig. 2 Temperature over time.

Throughout the annual cycle, Norway experiences a considerable spectrum of thermal variations, with minimum temperatures predominantly fluctuating between 0°C and 10°C. The most extreme temperature recorded was -22.2°C on February 28, 2018. Such drastic temperature variances underscore the nation's distinctive seasonal dichotomies, characterized by a pronounced thermal disparity between the frigid winters and the comparatively temperate summers.

p-ISSN 2798-253X
e-ISSN 2798-3153

Conversely, the maximum temperatures usually oscillate from 10°C to 30°C. The apex temperature documented in 2018 transpired on July 27, when the thermometer ascended to 31.4°C, delineating the zenith of the annual heat wave. This contrast between the temperatures experienced during summer and winter encapsulates Norway's formidable climatic challenges, influenced by its heterogeneous geographical characteristics and proximity to the Arctic region.

3.1. Predictive Modeling

In the execution of GRU analysis, it is imperative to standardize the data using a min-max scaler. Therefore, the dataset was partitioned into training and testing subsets. This study used 2,526 data points about minimum and maximum temperatures. The dataset was allocated 80% for training data, and 20% testing data. Specifically, 2,020 training data points spanning from February 1, 2018, to August 13, 2023, with the remaining 506 data points allocated for testing purposes. Moreover, the configuration of the number of timesteps to be considered was 3, indicating that the temperature prediction for the subsequent period utilized data from the preceding three days.

The parameters of the GRU architecture, as defined by the researcher, are comprehensively presented in Table 1. The configuration of the GRU model encompasses an input layer characterized by the number of time steps and the number of input features. It comprises two GRU layers, each consisting of 64 units and utilizing hyperbolic tangent (tanh) activation functions, interspersed with dropout layers (rate = 0.2) to alleviate the risk of overfitting. The initial GRU layer is designed to return sequences, whereas the subsequent layer does not. Following this, a dense layer with 32 units activated by the rectified linear unit (ReLU) function was included, culminating in an output dense layer (linear activation) that forecasts minimum and maximum temperatures. The model utilized the Adam optimization algorithm alongside the MSE as its loss function.

Table 1. Parameter of GRUs

Layer	Type	Unit/Nodes	Activation	Other Parameters
Input layer	Input	-	-	*n_steps*: the number of time steps *x_train.shape[2]*: the number of features (e.g., Min.Temp and Max.Temp)
Layer 1	GRU	64	tanh	*return_sequences=True* for passing to the next GRU layer
Dropout layer 1	Dropout	-	-	Rate: 0.2
Layer 2	GRU	64	tanh	*return_sequences*=False: the final recurrent layer
Dropout layer 2	Dropout	-	-	Rate: 0.2
Layer 3	Dense	32	ReLU	-
Output layer	Dense	*x_train.shape[2]*	Linear	Outputs Min.Temp and Max.Temp
Compilation	-	-	-	Optimizer: Adam Loss: Mean Squared Error

The model underwent training for 20 epochs utilizing a batch size of 32, thereby facilitating an equitable balance between computational efficiency and performance.

The configuration of critical parameters within the GRU model encompassing the number of timesteps (lookback duration), epochs, batch size, number of GRU units, and dropout rates were established through a rigorous methodology of hyperparameter optimization. In particular, a synthesis of empirical experimentation alongside validation performance assessment was implemented. The selection of a lookback duration of three days was predicated on initial exploratory analysis, which revealed that temperature fluctuations in Norway demonstrated considerable short-term autocorrelation so that a three-day interval proved effective for encapsulating vital temporal dependencies without excessively augmenting computational complexity.

Hyperparameters, including the number of epochs, batch size, GRU units, and dropout rate, were ascertained through iterative experimentation and the evaluation of model performance indicators, predominantly validation loss. The chosen configuration (20 epochs, a batch size of 32, 64 units per GRU layer, and a dropout rate of 0.2) represented an optimal equilibrium among model complexity, computational efficiency, and predictive accuracy. An escalation in the number of epochs or units

p-ISSN 2798-253X
e-ISSN 2798-3153

beyond this configuration yielded minimal enhancements in performance while concurrently elevating the risk of overfitting. Conversely, a reduction in epochs or units inadequately captured the intricacies of temperature variations.

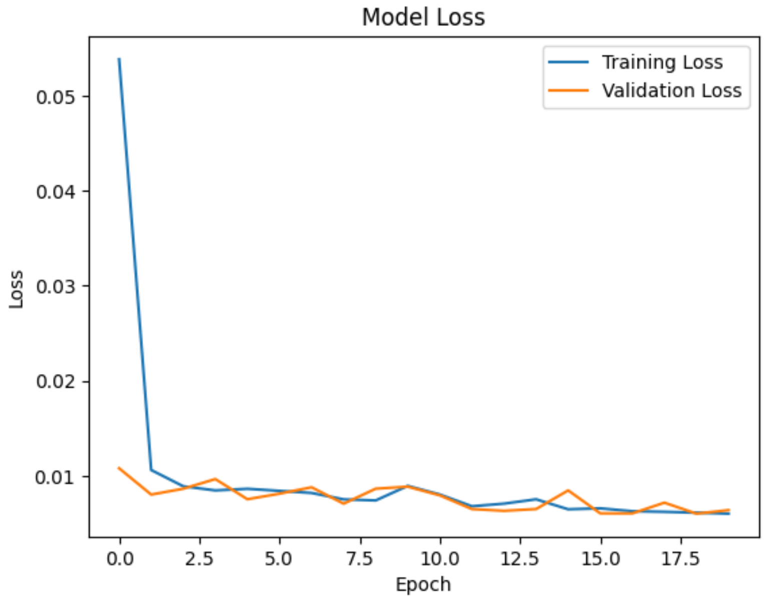

Fig. 3 Model loss for minimum temperature

In Fig. 3, the observed decline in training and validation losses during the initial epochs is substantial, indicating that the model is rapidly acquiring the capacity to reduce errors. Following approximately five epochs, both losses exhibit relative stability devoid of considerable overfitting (i.e., the training loss does not significantly fall below the validation loss). The continuous alignment of the validation loss with the training loss suggests that the model can generalize to previously unseen data without exhibiting significant overfitting.

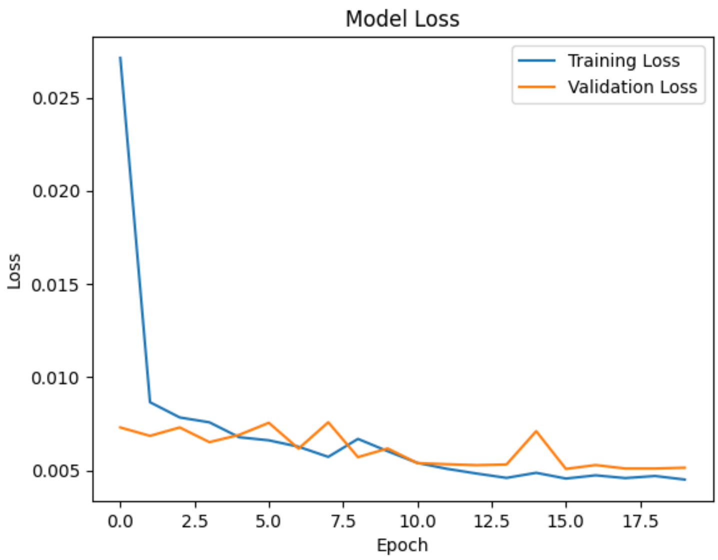

Fig. 4 Model loss for maximum temperature.

The discrepancy between the validation and training loss remained minimal throughout the epochs, implying that the model can generalize to previously unencountered data. Both loss metrics attained stabilization at relatively low magnitudes, and the terminal loss values were notably diminutive, signifying the model's commendable performance. Based on Fig. 4, the minor oscillation observed in the validation loss (for instance, around epoch 15) is characteristic and signifies the inherent variability in the model's performance on the validation dataset.

The evaluative metrics of the predictive model for minimum temperature exhibit a notable level of predictive accuracy. Specifically, for the training dataset, the MAE was recorded at 2.31, the MSE at 9.04, and the RMSE at 3.01, accompanied by a coefficient of R^2 of 0.82. In the context of maximum temperature data, the model demonstrated a slight enhancement, presenting an MAE of 2.21, an MSE of 8.62, an RMSE of 2.94, and an R^2 of 0.86. These findings imply that the model exhibits proficient generalization capabilities when applied to novel data, as evidenced by consistently low error rates and R^2 values indicating a robust correlation between the predicted and actual temperature values. The negligible discrepancy observed between the training and testing performance further substantiates the assertion that the model is not afflicted by overfitting, thereby establishing it as a dependable predictor for both minimum and maximum temperature outcomes.

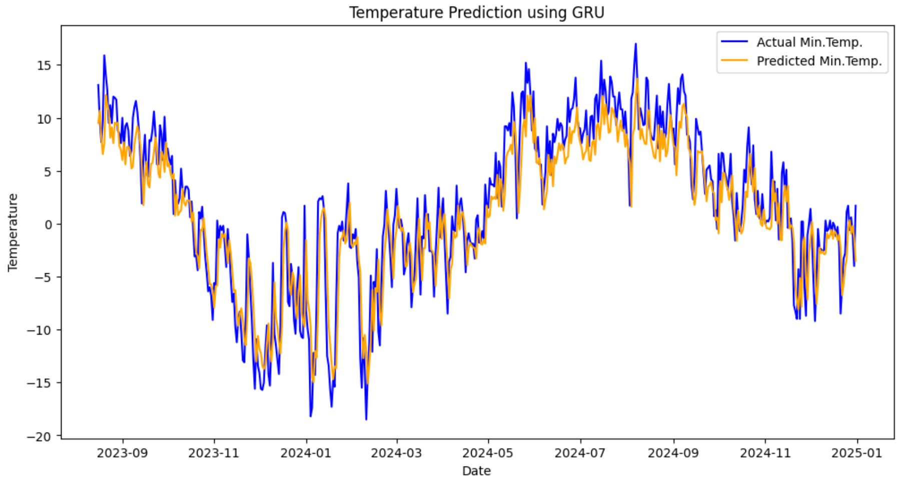

Fig. 5 Minimum temperature prediction.

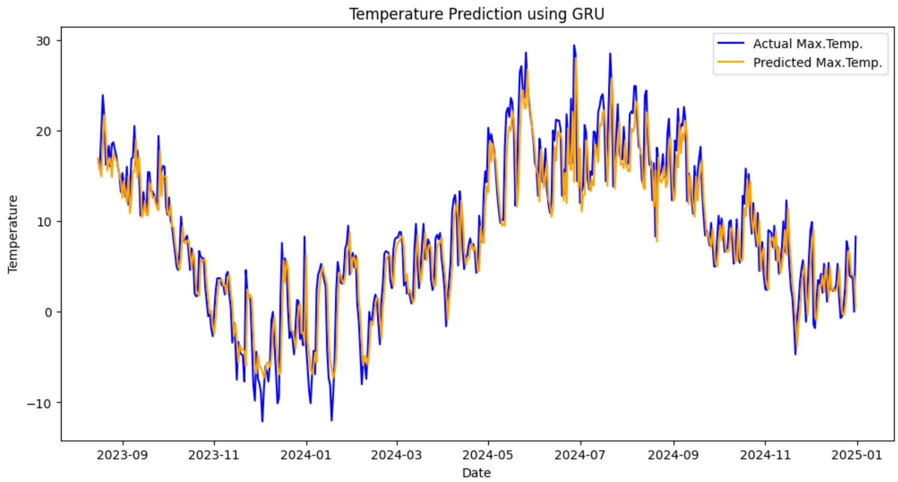

Fig. 6 Maximum temperature prediction.

Fig. 5 and Fig. 6 present graphical representations that delineate the efficacy of a GRU model in forecasting both minimum and maximum temperature values over a temporal continuum for validation datasets. Fig. 5 juxtaposes the actual minimum temperature readings (depicted in blue) against the model's projected values (illustrated in orange). In contrast, Fig. 6 offers a comparable analysis for maximum temperature readings. Both graphical depictions demonstrate a robust correspondence between the observed and projected values, indicating the model's adeptness in accurately capture seasonal patterns and temperature variations. The performance evaluation metrics substantiate this assertion, as evidenced by the low MAE, MSE, and RMSE values, indicating a

p-ISSN 2798-253X
e-ISSN 2798-3153

negligible divergence between the forecasts and the empirical data. The elevated R^2 coefficients (ranging from 0.82 to 0.85) signify that the model elucidates a considerable fraction of the variability inherent in the temperature dataset, thereby underscoring its proficiency in predicting temperature trends.

4. GRU Prediction for the Future

Since the GRU model demonstrates a high accuracy for training and testing data, it is well-suited for forecasting temperature. Therefore, it was used to predict temperature for 7 days, from January 1 until January 7, 2025 (Table 2).

Table 2. Temperature Prediction for Seven Days

Date	Minimum Temperature Prediction	Maximum Temperature Prediction
January 1, 2025	-3.52°C	0.45°C
January 2, 2025	-3.55°C	0.64°C
January 3, 2025	-3.76°C	0.53°C
January 4, 2025	-3.87°C	0.48°C
January 5, 2025	-3.96°C	0.45°C
January 6, 2025	-4.05°C	0.42°C
January 7, 2025	-4.13°C	0.38°C

The forecasts for the temperature during the first week of January 2025 predicted that Norway would encounter conventional winter climatic conditions. As illustrated in the meteorological predictions, the anticipated minimum temperature was projected to fluctuate between -3.52°C and -4.13°C, whereas the maximum temperature was expected to range from 0.38°C to 0.64°C. These temperature metrics are consistent with the winter season in Norway, which is typified by frigid temperatures, limited daylight hours, and frequent snowfall occurrences across various regions. The progressive decline in temperature throughout the seven-day timeframe implies a sustained cold trend, reinforcing the seasonal meteorological patterns anticipated during this year.

In practice, fine-tuning is typically preferred when revising an extant time-series model, owing to its computational efficiency and the robustness of the resultant outputs. A pretrained GRU model was utilized in the present investigation. Its training was extended over additional epochs with either exclusively novel data or a combination of recent historical data and the newly acquired dataset. This methodology substantially augments computational efficiency by capitalizing on previously acquired patterns, facilitating the model's rapid adaptation to contemporary data trends. However, the fine-tuning process necessitates meticulous oversight and validation protocols to guarantee that the model effectively assimilates new information while avoiding the pitfalls of overfitting and the potential deterioration of the generalization capabilities established during the initial training phase.

5. Conclusion

The GRU model has been successfully utilized to develop a predictive model for average minimum and maximum temperatures based on time series data. Multiple experiments evaluating performance metrics on training and test datasets conclude that the GRUs model, trained on 2020 observations and tested on 526 data points, provides reliable temperature predictions. Using a 20-epoch training process and considering data from the previous three days to predict the next day's temperature, the model achieved an R^2 score of 0.82 for minimum and 0.86 for maximum temperatures. These results demonstrate the GRU model's effectiveness in capturing daily temperature fluctuations and making accurate forecasts.

References

[1] D.K. Roy, M.A. Hossain, M.P. Haque, A. Alataway, A.Z. Dewidar, and M.A. Mattar, "Automated model selection using Bayesian optimization and the asynchronous successive halving algorithm for predicting daily minimum and maximum temperatures," *Agriculture*, vol. 14, no. 2, Feb. 2024, Art. no 278, doi: 10.3390/agriculture14020278.

[2] J. Oliver, "Norway's climate odyssey: Assessing impacts, mitigation strategies, and policy responses in a warming Arctic," *Endless Int. J. Future Stud.*, vol. 6, no. 3, pp. 29–43, Sep. 2023, doi: 10.54783/endlessjournal.v6i3.198.

[3] F. Akcakoca and H. Apaydin, "Modelling of Bektas Creek daily streamflow with generalized regression neural network method," *Int. J. Adv. Sci. Res. Eng.*, vol. 6, no. 2, pp. 97–103, Feb. 2020, doi: 10.31695/IJASRE.2020.33717.

[4] F. Xie, H. Yan, Y. Long, H. Guo, H. Liu, and P. Yu, "Weather prediction based on multivariate LSTM neural network model," in *Intelligent Computing Technology and Automation* (Advances in Transdisciplinary Engineering Series 47), Z. Hou, Ed., Amsterdam, Netherland: IOS Press BV, 2024, pp. 298–303, doi: 10.3233/ATDE231201.

[5] C. Wang, P. Wang, P. Wang, B. Xue, and D. Wang, "Using conditional generative adversarial 3-D convolutional neural network for precise radar extrapolation," *IEEE. J. Sel. Top. Appl. Earth Obs. Remote Sens.*, vol. 14, pp. 5735–5749, 2021, doi: 10.1109/JSTARS.2021.3083647.

[6] F. Wang, D. Zhang, G. Min, and J. Li, "Reservoir production prediction based on variational mode decomposition and gated recurrent unit networks," *IEEE Access*, vol. 9, pp. 53317–53325, 2021, doi: 10.1109/ACCESS.2021.3070343.

[7] F.R. Alharbi and D. Csala, "Short-term wind speed and temperature forecasting model based on gated recurrent unit neural networks," in *2021 3rd Global Power Energy Commun. Conf. (GPECOM)*, Oct. 2021, pp. 142–147, doi: 10.1109/GPECOM52585.2021.9587479.

[8] X. Wang et al., "Sparse data-extended fusion method for sea surface temperature prediction on the East China Sea," *Appl. Sci.*, vol. 12, no. 12, Jun. 2022, Art. no 5905, doi: 10.3390/app12125905.

[9] D.F. Godoy-Rojas et al., "Attention-based deep recurrent neural network to forecast the temperature behavior of an electric arc furnace side-wall," *Sensors*, vol. 22, no. 4, Feb. 2022, Art. no 1418, doi: 10.3390/s22041418.

[10] T. Sivakumar, P.T. Suraj, and P.C. Jayashree, "Trends in climatic change in the last 50 years at Seven Agro-climatic regions of Tamil Nadu," in *Climate Change Modelling, Planning and Policy for Agriculture*, A.K. Singh, J.C. Dagar, A. Arunachalam, and G.R.K Shelat (Eds.). New Delhi, India: Springer India, 2015, pp. 187–198, doi: 10.1007/978-81-322-2157-9_19.

[11] A. Panda and N. Sahu, "Trend analysis of seasonal rainfall and temperature pattern in Kalahandi, Bolangir and Koraput districts of Odisha, India," *Atmospheric Sci. Lett.*, vol. 20, no. 10, Oct. 2019, doi: 10.1002/asl.932.

[12] J. Abaurrea, J. Asín, and A.C. Cebrián, "Modelling the occurrence of heat waves in maximum and minimum temperatures over Spain and projections for the period 2031-60," *Glob Planet Change*, vol. 161, pp. 244–260, Feb. 2018, doi: 10.1016/j.gloplacha.2017.11.015.

[13] D. O'Shaughnessy, "Trends and developments in automatic speech recognition research," *Comput. Speech Lang.*, vol. 83, p. 101538, Jan. 2024, doi: 10.1016/j.csl.2023.101538.

[14] J. Chung, C. Gulcehre, K. Cho, and Y. Bengio, "Empirical evaluation of gated recurrent neural networks on sequence modeling," 2014, *arXiv: 1412.3555v1*.

[15] O. Kaypakli and M. Özgeyik, "The effect of heart rate and pulse pressure on mean arterial pressure: the combined formula for calculation of mean arterial pressure," *Blood Press. Monit.*, vol. 26, no. 5, pp. 373–379, Oct. 2021, doi: 10.1097/MBP.0000000000000548.

[16] A.F. Saad and Z.I. Elghobary, "Theoretical predictions of nuclear binding energy for the observed nuclei: the influence of coefficients and terms in a semi-empirical mass formula," *Phys. Scr.*, vol. 99, no. 8, Aug. 2024, Art. no 99 085308, doi: 10.1088/1402-4896/ad6198.

[17] Y. Sun, Y. Polyanskiy, and E. Uysal, "Sampling of the Wiener process for remote estimation over a channel with random delay," *IEEE Trans. Inf. Theory*, vol. 66, no. 2, pp. 1118–1135, Feb. 2020, doi: 10.1109/TIT.2019.2937336.

[18] G. Hexner and H. Weiss, "An extended Kalman filter with a computed mean square error bound," in *53rd IEEE Conf. Decis. Control*, Dec. 2014, pp. 5008–5014, doi: 10.1109/CDC.2014.7040171.

[19] S. Kotaška, D. Duchan, P. Pelikán, and M. Špano, "Spectral analysis of oscillatory wind wave parameters in fetch-limited deep-water conditions at a small reservoir and their prediction: Case study of the Hulín Reservoir in the Czech Republic," *J. Hydrol. Hydromech.*, vol. 72, no. 1, pp. 95–112, Mar. 2024, doi: 10.2478/johh-2023-0042.

[20] N. Ichihara et al., "Achieving clinically optimal balance between accuracy and simplicity of a formula for manual use: Development of a simple formula for estimating liver graft weight with donor

anthropometrics," *PLoS One*, vol. 18, no. 1, Jan. 2023, Art. no e0280569, doi: 10.1371/journal.pone.0280569.

[21] L. Kusumawati, E. Setyowati, and A.B. Purnomo, "Practical-empirical modeling on envelope design towards sustainability in tropical architecture," *Sustainability*, vol. 13, no. 5, Mar. 2021, Art. no 2959, doi: 10.3390/su13052959.

p-ISSN 2798-253X
e-ISSN 2798-3153